

# The Benzene–Argon Ground-State Intermolecular Potential Energy Surface Revisited

**Silvia Bouzón Capelo and Berta Fernández**

*Department of Physical Chemistry, Faculty of Chemistry, University of Santiago de Compostela, E-15782 Santiago de Compostela, Spain*

**Henrik Koch**

*Department of Chemistry, Norwegian University of Science and Technology, N-7491 Trondheim, Norway*

**Peter M. Felker**

*Department of Chemistry and Biochemistry, University of California, Los Angeles, California 90095-1569*

*Received: February 10, 2009; Revised Manuscript Received: March 10, 2009*

The benzene–Ar ground-state  $S_0$  intermolecular potential energy surface is evaluated using the coupled cluster singles and doubles model including connected triple corrections and the augmented correlation consistent polarized valence triple- $\zeta$  basis set extended with a set of 3s3p2d1f1g midbond functions. The surface is characterized by absolute minima of  $-390.1 \text{ cm}^{-1}$  where the argon atom is located on the benzene  $C_6$  axis at distances of  $\pm 3.536 \text{ \AA}$ , and has a general shape close to the available ground-state  $S_0$  and the first singlet  $S_1$  and triplet  $T_1$  excited-state surfaces. Using the potential, the intermolecular level structure of the complex is evaluated. The new intermolecular potential energy surface gives very accurate results and improves those previously available.

## 1. Introduction

Van der Waals complexes play a major role in physics, chemistry, and biology.<sup>1–3</sup> They are characterized by an interaction dominated by dispersion, interaction that is essential in processes like the solvation or adsorption of molecules. Therefore, van der Waals complexes are used as models for the study of this type of processes.<sup>4</sup> Complexes formed by an aromatic molecule and noble gas atoms have been the focus of a considerable number of studies. Series of systems constituted by an aromatic molecule to which a successive number of rare-gas atoms are added were studied as models for different solvation steps.<sup>5,6</sup> In particular, the benzene–Ar complex has been a focus of major attention, both from the experimental and the theoretical points of view.<sup>7,8</sup>

Within the experimental work, complexes involving aromatic molecules have mainly been investigated using high resolution spectroscopy.<sup>9</sup> We cite here the work of Brupbacher et al.<sup>10</sup> where an empirical intermolecular potential was derived for the benzene–Ar complex from the rotational spectra measured in microwave experiments. This potential gave very good agreement with the lower vibrational states of the complex. The studies of Kim and Felker<sup>11</sup> and Neuhauser et al.<sup>12</sup> are also worthwhile mentioning. The former measured the five lowest vibrational transitions by nonlinear Raman spectroscopy with a resolution of  $0.03 \text{ cm}^{-1}$ . Neuhauser et al. reported six of the lower vibrational states determined by coherent ion dip spectroscopy. The high accuracy of these results is a challenge for the theoretical description of the complex. In ref 13 a review on previous experimental studies available on the complex is given.

The theoretical description of van der Waals complexes is very demanding in terms of high-quality correlation methods

and large basis sets. From the theoretical point of view the stability of the benzene–Ar complex is completely due to correlation effects. Methods like the self consistent field (SCF), density functional theory (DFT) or even Möller–Plesset MP2 are unable to describe the interaction.

We have carried out the theoretical evaluation of a considerable number of van der Waals complex intermolecular potential energy surfaces (IPESs) (see ref 14 and references cited therein). We started the studies by selecting an adequate method and basis set, evaluating the benzene–argon dissociation energies in the ground and in the first singlet excited-state using different methods (DFT, SCF, MP2, coupled cluster singles and doubles (CCSD) and coupled cluster singles and doubles including connected triple corrections (CCSD(T))); and basis sets in Dunning's series<sup>15</sup> and comparing the results with the accurate experimental data available. The efficient performance of the CCSD(T) method together with the aug-cc-pVDZ-33211 basis set, i.e. the aug-cc-pVDZ basis set extended with a set of 3s3p2d1f1g midbond functions<sup>16,17</sup> (denoted 33211 in the following), was clearly shown.<sup>8</sup> Therefore, we decided to use this basis set and method in the evaluation of the different ground-state IPESs. The good performance was corroborated when comparing the spectra obtained from the theoretical surfaces with the experimental results available.

For a detailed description on previous theoretical benzene–argon theoretical IPESs see refs 13, 18, and 19. The most accurate benzene–argon ground-state surface available has been obtained from CCSD(T) aug-cc-pVDZ-33211 interaction energies.<sup>13</sup> It is characterized by two equivalent minima ( $-387.0 \text{ cm}^{-1}$ ), where the argon atom is located on the benzene  $C_6$  axis at distances of  $\pm 3.555 \text{ \AA}$  and six equivalent very flat minima in the benzene plane. The  $S_1$  potential has been evaluated with the same basis set and the CCSD and CCSD(T) methods and it has a shape similar to that of the ground state, with minima

Author for correspondence. E-mail: qfberta@usc.es.

( $-415.1 \text{ cm}^{-1}$ ) at distances of  $\pm 3.490 \text{ \AA}$ .<sup>18</sup> The IPESs were used in full three-dimensional dynamical calculations to obtain the vibrational energy levels. For the ground and the first singlet excited states very accurate experimental work has been carried out and precise results on the vibrational spectra are available. The theoretical results agreed well with the experimental data and even allowed to correct the experimental assignments.<sup>13</sup> For the singlet excited-state the agreement was worse, but still satisfactory. Considering this good performance, we also carried out the evaluation of the triplet  $T_1$  excited-state surface using the CCSD and the CCSD(T) methods.<sup>19</sup> This surface is characterized by absolute minima of  $-392.5 \text{ cm}^{-1}$ , where the argon atom is located on the benzene  $C_6$  axis at distances of  $\pm 3.515 \text{ \AA}$ . Due to the lack of experimental data on the triplet surface, the results of the study were predictive.

The aim of the present work is to improve the ground-state surfaces available, by going a step further and using Dunning's aug-cc-pVTZ basis set<sup>15</sup> extended with a set of 3s3p2d1f1g midbond functions (denoted aug-cc-pVTZ-33211) in the calculations. Considering the basis set study we have carried out in ref 13 for the benzene-argon interaction energies, we can expect improvements of a few  $\text{cm}^{-1}$  in the interaction energies around the minima, and larger at longer distances. After obtaining the surface, we evaluate the spectroscopic properties.

This paper is organized as follows: In section 2 we describe the computational details and discuss and analyze the IPES, comparing the results with those already available in the literature, in section 3 we will follow a parallel approach for the intermolecular level analysis and in the last section we summarize and give our concluding remarks.

## 2. Intermolecular Potential Energy Surface

In order to construct the IPES, we start by evaluating 108 points on the potential energy surface, using the CCSD(T) method<sup>20–22</sup> and the aug-cc-pVTZ-33211 basis set. The mid-bond functions have exponents of 0.9, 0.3, and 0.1 for the s and the p functions, 0.6 and 0.2 for the d, and 0.3 for the f and the g function; and located in the middle of the van der Waals bond are well-known to improve the basis set convergence efficiency.<sup>16</sup> The energies are evaluated as the difference between the complex energy and the energies of the monomers, and corrected for the basis set superposition error through the counterpoise method.<sup>23</sup>

To evaluate the ground-state interaction energies we keep the benzene geometry fixed at the most accurate experimental value available ( $R_{CC} = 1.397 \text{ \AA}$  and  $R_{CH} = 1.080 \text{ \AA}$ ).<sup>7</sup> As intermolecular coordinates we use the  $(x, y, z)$  Cartesian coordinates of the Ar atom position vector  $\vec{r}$  with the origin in the benzene center of mass. The  $z$  axis of the coordinate axis system is the  $C_6$  symmetry axis of benzene, and the  $x$  axis lies in the benzene plane and is directed to one of the benzene carbon atoms. The  $y$  axis is perpendicular to the  $x$  and  $z$  axes and passes through a C–C bond. The results are given in the Supporting Information.

The IPES is generated from the *ab initio* interaction energies by fitting the function  $V(x, y, z)$  to the determined points. We consider all the interaction energies lower than  $300 \text{ cm}^{-1}$ . A many-body expansion of  $V(x, y, z)$  has been successfully employed previously to fit the *ab initio* data for the electronic ground<sup>13</sup> and first excited singlet<sup>18</sup> and triplet<sup>19</sup> states of the benzene–Ar complex. The same expansion up to four-body terms is used here:

$$V(\vec{r}) = W_0 \left[ \sum_k V_2(r_k) + \sum_{l < k} V_3(r_k, r_l) + \sum_{m < l < k} V_4(r_k, r_l, r_m) \right] \quad (2)$$

where

$$r_k = [(x - X_k)^2 + (y - Y_k)^2 + b_z(z - Z_k)^2]^{1/2} \quad (3)$$

is a modified distance between Ar and the benzene  $k$ th atom placed at  $\vec{R}_k = (X_k, Y_k, Z_k)$ . The effect of the hydrogen atoms is effectively included in the carbons, taking this into account, the coordinates are calculated with  $R_{C-C} = 1.395 \text{ \AA}$ . The coefficient  $b_z$  takes into account an essential part of the IPES anisotropy, neglected by omission of the hydrogens in the sums of eq 2.

The two-body potential term  $V_2$  is expanded in the Morse form

$$V_2(r_k) = w^2(r_k) + \sum_{i=3}^5 c_i w^i(r_k) + c_6 \tilde{w}^6(r_k) \quad (4)$$

where

$$w(r_k) = 1 - \exp(-a(r_k - r_0)) \quad (5)$$

For the last term  $w(r_k)$  is replaced by a modified term

$$\tilde{w}(r_k) = w(r_k) \text{ for } r_k \geq r_0 \text{ and } \tilde{w}(r_k) = 0 \text{ for } r_k < r_0 \quad (6)$$

describing only the attractive part of the interaction. The repulsive part in this term is replaced by zero. The term  $\tilde{w}(r_k)$  is introduced to prevent the IPES from growing too sharply in the region of very small values of  $r_k$ .

The three-body term is given by:

$$V_3(r_k, r_l) = \sum_i c_{ii} w^i(r_k) w^i(r_l) + \sum_{i < j} c_{ij} (w^i(r_k) w^j(r_l) + w^i(r_l) w^j(r_k)) \quad (7)$$

and the four-body:

$$\begin{aligned} V_4(r_k, r_l, r_m) = & c_{111} w(r_k) w(r_l) w(r_m) \\ & + c_{112} (w(r_k) w(r_l) w^2(r_m) + w(r_m) w(r_k) w^2(r_l) + \\ & \quad w(r_l) w(r_m) w^2(r_k)) \\ & + c_{122} (w(r_k) w^2(r_l) w^2(r_m) + w(r_m) w^2(r_k) w^2(r_l) + \\ & \quad w(r_l) w^2(r_m) w^2(r_k)) \\ & + c_{113} (w(r_k) w(r_l) w^3(r_m) + w(r_m) w(r_k) w^3(r_l) + \\ & \quad w(r_l) w(r_m) w^3(r_k)) \quad (8) \end{aligned}$$

In the Supporting Information the errors of the analytic potential function  $V$ -390  $\text{cm}^{-1}$  fitted to the *ab initio* energies are shown. The fitted IPES reproduces the *ab initio* values with a maximum error of  $0.615 \text{ cm}^{-1}$ . This error is comparable to what we obtained previously for the corresponding aug-cc-pVDZ-33211 IPES.<sup>13</sup> The fitted values of the IPES parameters are given in Table 1.

The contour plots of the IPES are shown in Figure 1. The stationary points are reported in Table 2, where the values are compared to those of the previous  $S_0$ ,  $S_1$  and  $T_1$  *ab initio* potentials available. The general shape of the aug-cc-pVTZ-33211 IPES is similar to that of the aug-cc-pVDZ-33211 ground-state IPES.<sup>13</sup> The more accurate surface corrects the values of the minima by a few  $\text{cm}^{-1}$  and improves the long-range domain, where differences up to  $60 \text{ cm}^{-1}$  are found.

**TABLE 1: Parameters of the Analytic IPES Fitted to the *ab Initio* Interaction Energies<sup>a</sup>**

potential parameters	
$r_0/\text{\AA}$	4.1576185
$a/\text{\AA}^{-1}$	0.61457753
$b_z$	1.2267881
$W_0/\text{cm}^{-1}$	846.74834
$c_3$	-1.3886642
$c_4$	0.84691619
$c_5$	-1.8145219
$c_6$	-0.0057453988
$c_{11}$	-0.23523780
$c_{12}$	0.23006600
$c_{22}$	-2.3897651
$c_{13}$	0.35230481
$c_{14}$	1.1196152
$c_{23}$	0.40888796
$c_{111}$	-0.10273306
$C_{112}$	0.36480456
$c_{122}$	0.58991483
$c_{113}$	-1.1757265

<sup>a</sup> The value of the IPES is zero at the minimum.

### 3. Calculation of Benzene–Ar Intermolecular Level Structure

The  $J = 0$  level structure corresponding to the fitted IPES is computed variationally in the rigid monomer approximation by using the procedure described in ref 24. Only the values of various basis-set and potential-energy grid parameters differ in this work relative to those of that paper. Specifically, the basis-set and grid sizes employed here are about twice as large as those of the prior work. Calculations are performed for perprotonated and perdeuterated benzene–Ar. For the two isotopomers we take the benzene masses to be 78.047 and 84.084 amu, respectively, and the benzene in-plane moments of inertia to be 88.7846 and 107.398 amu·Å<sup>2</sup>, respectively. The benzene moments of inertia along the  $C_6$  axis are taken to be two-times those of the in-plane moments. The Ar mass is taken to be 39.95 amu.

Tables 3 and 4 present intermolecular frequencies for perprotonated and perdeuterated benzene–Ar, respectively. In each table three sets of calculated results and two sets of experimental results appear. The former correspond to the IPES of this work, the IPES based on the CCSD(T) aug-cc-pVDZ-33211 *ab initio* results of ref 13, and the empirically derived IPES of ref 10. The latter are stimulated Raman results pertaining to intermolecular transitions built off of the  $S_0$  zero-point level of the complex<sup>11</sup> and coherent ion dip results pertaining to intermolecular transitions built off of the benzene-localized  $6_2$  vibrational level in  $S_0$ .<sup>12</sup> Both calculated and observed frequencies are assigned to quanta of the doubly degenerate intermolecular bending mode ( $\beta$ ) and the nondegenerate intermolecular stretching mode ( $\sigma$ ). The number of quanta of each pertaining to a given frequency is denoted as a subscript to  $\beta$  and  $\sigma$ , respectively.

Two main points are evident from comparison of the calculated and observed results. First, all three of the IPES give rise to  $\sigma$  intervals that are too small by slightly over 1%. Second, the two *ab initio* IPESs do a better job in handling states with nonzero bending quanta than does the empirical IPES (though there is not much difference in performance between the *ab initio* surfaces). This is particularly evident in comparison of the calculated and measured frequencies for the  $\beta_2(A_1) \leftrightarrow 0_0$  intervals of both isotopomers. Indeed, at least for the lower-energy  $\beta_n$  intervals, the *ab initio* surfaces produce results accurate to well under 1%.

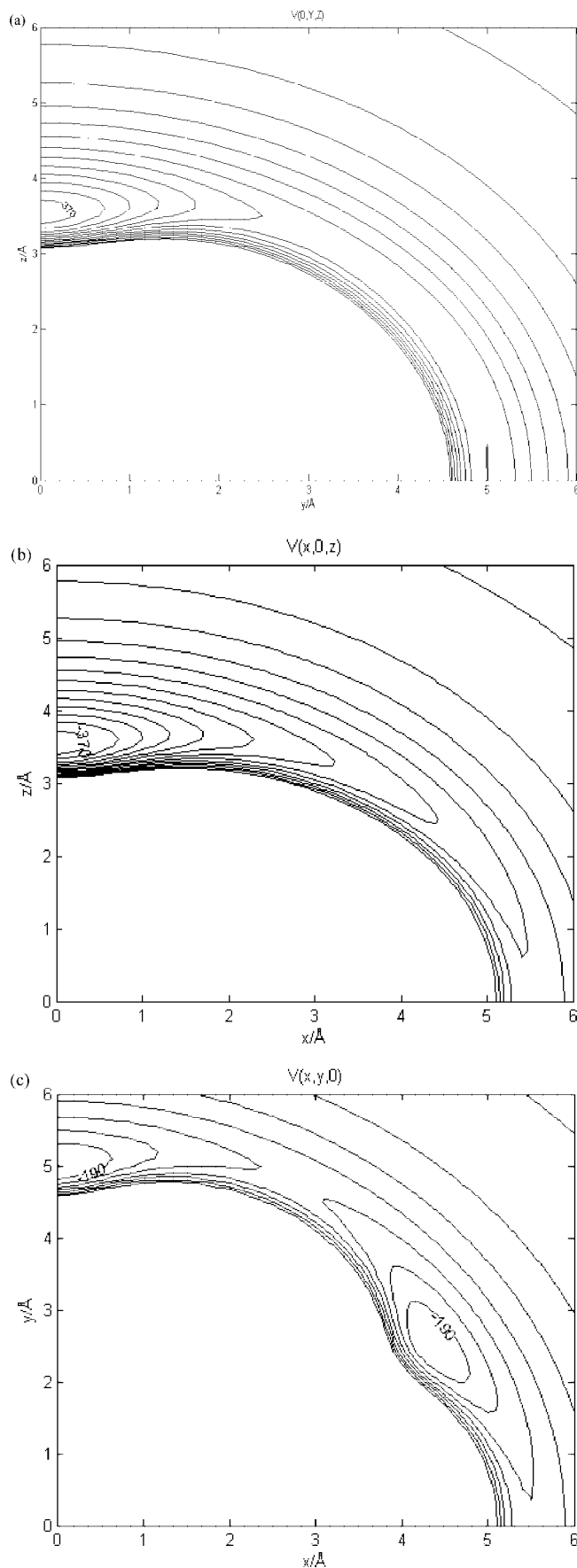


**Figure 1.** Contour plots of the *ab initio* IPES fitted by the analytic function with the parameters specified in Table 2 In the  $yz$  plane (a), in the  $xz$  plane (b), in the  $xy$  plane (c). The values of subsequent contours differ by 30  $\text{cm}^{-1}$ .

**TABLE 2: Stationary Points of the aug-cc-pVTZ-33211  $S_0$  Electronic State IPES<sup>a</sup>**

state	minimum		minimum		saddle point			saddle point	
	(0,0, $z_e$ )		(0, $y_m$ ,0)		(0, $y_s,z_s$ )			( $x_s$ ,0,0)	
	$z_e$	$V_e$	$y_m$	$V_m$	$y_s$	$z_s$	$V_s$	$x_s$	$V_s$
$S_0^b$	3.5357	0.0	5.0125	169.5	3.3500	3.0440	180.5	5.5004	261.1
$S_0^c$	3.5547	0.0	5.0289	170.0	3.4247	3.0163	183.8	5.5215	263.8
$S_1^d$	3.4896	0.0	5.0505	191.8	3.8080	2.6938	204.7	5.5628	288.4
$T_1^e$	3.5153	0.0	5.0491	170.0	3.8602	2.6572	186.57	5.5562	264.8
exp. <sup>f</sup>		0.0							

<sup>a</sup> Results are compared to previous results for  $S_0$ ,  $S_1$ , and  $T_1$  and the experimental values; the coordinates are in Å and energies  $V$ , measured from the bottom of the potential  $V_0$ , in  $\text{cm}^{-1}$ . <sup>b</sup>  $V_0 = -390.1 \text{ cm}^{-1}$ . <sup>c</sup> aug-cc-pVDZ-33211 IPES, ref 13  $V_0 = -387.0 \text{ cm}^{-1}$ . <sup>d</sup> aug-cc-pVDZ-33211 IPES, ref 18  $V_0 = -415.1 \text{ cm}^{-1}$ . <sup>e</sup> aug-cc-pVDZ-33211 IPES, ref 19,  $V_0 = -392.5 \text{ cm}^{-1}$ . <sup>f</sup>  $V_0 < 390 \text{ cm}^{-1}$ . Evaluated from the  $D_0$  upper limit of  $340 \text{ cm}^{-1}$  reported by Krause et al.<sup>28</sup> and the corresponding vibrational ground-state energy ( $50 \text{ cm}^{-1}$ ).<sup>29</sup>

**TABLE 3: Calculated and Measured Intermolecular Frequencies ( $\text{cm}^{-1}$ ) for Perprotonated Benzene–Ar**

$\Gamma$ ( $C_{6v}$ )	assignment	$E(\text{fit})^a$	$E(\text{fit})^b$	$E(\text{fit})^c$	$E(\text{exp})^d$	$E(\text{exp})^e$
$A_1$	$0_0$	0	0	0		
$E_1$	$\beta_1$	33.1	33.2	33.1	33.0	32.8
$A_1$	$\sigma_1$	39.5	39.5	39.6	39.9	40.0
$E_2$	$\beta_2$	63.3	63.7	63.4	63.3	
$A_1$	$\beta_2$	65.3	65.6	66.4	65.5	65.4
$E_1$	$\beta_1\sigma_1$	68.2	68.4	68.3	68.7	
$A_1$	$\sigma_2$	76.2	76.2	76.4		77.1
$B_1$	$\beta_3$	90.5	91.1	91.1		
$B_2$	$\beta_3$	90.7	91.3	91.2		
$E_1$	$\beta_3$	93.9	94.5	96.0		
$E_2$	$\beta_2\sigma_1$	94.0	94.5	94.8		
$A_1$	$\beta_2\sigma_1$	95.6	96.0	97.4		96.0
$E_1$	$\beta_1\sigma_2$	101.4	101.7	102.2		
$A_1$	$\sigma_3$	109.8	109.8	110.2		
$E_2$	$\beta_4$	114.8	115.7	116.4		(117.2) <sup>f</sup>
$B_1$	$\beta_3\sigma_1$	116.5	117.3	118.8		
$B_2$	$\beta_3\sigma_1$	117.0	117.8	119.2		
$E_2$	$\beta_4$	117.9	118.7	121.2		
$E_1$	$\beta_3\sigma_1$	119.0	119.7	122.8		
$A_1$	$\beta_4$	119.4	120.0	123.4		
$E_2$	$\beta_2\sigma_2$	125.4	125.9	127.6		
$A_1$	$\beta_2\sigma_2$	127.5	127.9	130.5		(128.2) <sup>f</sup>
$E_1$	$\beta_1\sigma_3$	131.0	131.4	132.8		

<sup>a</sup> IPES from this work. Frequencies are relative to the zero-point level  $58.81 \text{ cm}^{-1}$  above the IPES minimum, which is  $390.08 \text{ cm}^{-1}$  below the dissociation threshold. <sup>b</sup> IPES from ref 13. Frequencies are relative to the zero-point level  $58.9 \text{ cm}^{-1}$  above the IPES minimum, which is  $387.0 \text{ cm}^{-1}$  below the dissociation threshold. <sup>c</sup> IPES from ref 10. Frequencies are relative to the zero-point level  $59.24 \text{ cm}^{-1}$  above the IPES minimum, which is  $408 \text{ cm}^{-1}$  below the dissociation threshold. <sup>d</sup> Data for the  $S_0 0_0$  state from ref 11. <sup>e</sup> Data for the  $S_0 6_2$  state from ref 12. <sup>f</sup> The assignments we have indicated for measured frequencies in parentheses are tentative and differ from the assignments made originally in ref 12.

Considering the results for the zero-point energy levels, an improvement of about  $3 \text{ cm}^{-1}$  is obtained in the  $D_0$  energy when going from the aug-cc-pVDZ-33211 to the aug-cc-pVTZ-33211 results. In this way,  $D_0$  gets closer to the  $D_0$  upper limit of  $340 \text{ cm}^{-1}$  reported by Krause et al.<sup>25</sup>

We also calculate the rotational constants of the two benzene–Ar isotopomers for the fitted IPES presented here. The calculations are performed according to the procedure described in ref 26 and involve computing the energies of excited rotational levels by suitable transformation of  $J = 0$  eigenstates to an Eckart body-fixed frame. Table 5 presents the results of these calculations for the six lowest intermolecular vibrational states in each isotopomer. Unfortunately, the only  $S_0$  experimental results that we know of are for the  $0_0$  levels (e.g., ref 27). Moreover, (a) only the B rotational constants for

**TABLE 4: Calculated and Measured Intermolecular Frequencies ( $\text{cm}^{-1}$ ) for Perdeuterated Benzene–Ar**

$\Gamma$ ( $C_{6v}$ )	assignment	$E(\text{fit})^a$	$E(\text{fit})^b$	$E(\text{fit})^c$	$E(\text{exp})^d$	$E(\text{exp})^e$
$A_1$	$0_0$	0	0	0		
$E_1$	$\beta_1$	30.9	31.0	30.9	30.9	30.2
$A_1$	$\sigma_1$	39.2	39.2	39.1	39.6	39.6
$E_2$	$\beta_2$	59.4	59.7	59.4	59.5	
$A_1$	$\beta_2$	61.5	61.7	62.5	61.6	61.5
$E_1$	$\beta_1\sigma_1$	65.9	66.1	65.9	66.3	
$A_1$	$\sigma_2$	75.4	75.4	75.3		76.1
$B_1$	$\beta_3$	85.2	85.8	85.6		
$B_2$	$\beta_3$	85.4	85.9	85.8		
$E_1$	$\beta_3$	89.2	89.6	90.9		
$E_2$	$\beta_2\sigma_1$	90.2	90.7	90.7		
$A_1$	$\beta_2\sigma_1$	92.3	92.7	93.7		92.6
$E_1$	$\beta_1\sigma_2$	98.4	98.6	98.7		
$A_1$	$\sigma_3$	108.3	108.4	108.4		
$E_2$	$\beta_4$	108.6	109.4	109.7		
$B_1$	$\beta_3\sigma_1$	111.8	112.6	113.5		
$B_2$	$\beta_3\sigma_1$	112.2	113.0	113.8		
$E_2$	$\beta_4$	113.3	114.0	115.9		
$E_1$	$\beta_3\sigma_1$	115.3	115.9	118.2		(115.6) <sup>f</sup>
$A_1$	$\beta_4$	115.4	115.9	118.6		
$E_2$	$\beta_2\sigma_2$	120.0	120.5	121.6		
$A_1$	$\beta_2\sigma_2$	122.3	122.7	124.7		
$E_1$	$\beta_1\sigma_3$	127.4	127.9	128.8		

<sup>a</sup> IPES from this work. Frequencies are relative to the zero-point level  $56.00 \text{ cm}^{-1}$  above the IPES minimum. <sup>b</sup> IPES from ref 13. Frequencies are relative to the zero-point level  $56.06 \text{ cm}^{-1}$  above the IPES minimum. <sup>c</sup> IPES from ref 10. Frequencies are relative to the zero-point level  $56.37 \text{ cm}^{-1}$  above the IPES minimum. <sup>d</sup> Data for the  $S_0 0_0$  state from ref 11. <sup>e</sup> Data for the  $S_0 6_2$  state from ref 12. <sup>f</sup> The assignments we have indicated for measured frequencies in parentheses are tentative and differ from the assignments made originally in ref 12.

the two isotopomers have been extracted by fitting to experimental results, and (b) the fits have been performed by constraining the relevant A constant to be equal to C for bare benzene. Within these limits, though, one sees that the calculated  $0_0$  values agree well with the experimental values. One also notes that the variation in calculated A values as a function of intermolecular state suggests that the assumption that  $A(\text{Benzene} - \text{Ar}) = C(\text{Benzene})$  is likely only accurate to within about a percent of A.

#### 4. Summary and Conclusions

We evaluate the benzene–Ar ground-state  $S_0$  IPES using the CCSD(T) method and the aug-cc-pVTZ-33211 basis set. The surface presents absolute minima of  $-390.1 \text{ cm}^{-1}$  with the argon atom located on the benzene  $C_6$  axis at distances of  $\pm 3.536 \text{ Å}$ , and a general shape close to the ground-state  $S_0$  and the first

**TABLE 5: Calculated and Measured Rotational Constants ( $\text{cm}^{-1}$ ) for Perprotonated and Perdeuterated Benzene–Ar**

vibrational state	A	B	$2\xi A$
	h6		
$0_0$	0.09562 (0.09488) <sup>a</sup>	0.03897 (0.03937) <sup>b</sup>	0
$\beta_1$	0.09643	0.03816	0.03973
$\sigma_1$	0.09562	0.03897	0
$\beta_2(\text{E}_2)$	0.09740	0.03729	0.07975
$\beta_2(\text{A}_1)$	0.09723	0.03728	0
$\beta_1\sigma_1$	0.09711	0.03702	0.03930
	d6		
$0_0$	0.007901 (0.07851) <sup>a</sup>	0.03684 (0.03708) <sup>b</sup>	0
$\beta_1$	0.07963	0.03614	0.03734
$\sigma_1$	0.07927	0.03586	0
$\beta_2(\text{E}_2)$	0.08035	0.03539	0.07471
$\beta_2(\text{A}_1)$	0.08019	0.03539	0
$\beta_1\sigma_1$	0.08017	0.03510	0.03686

<sup>a</sup> The values for A were not measured but were assumed to be equal to the measured value for the out-of-plane rotational constant (C) of bare benzene isotopomer. See ref 27 for details. <sup>b</sup> From ref 27. Note that the reported values were obtained by fitting to experimental results under the assumption that A for the complex is equal to C for the bare benzene isotopomer.

singlet  $S_1$  and triplet  $T_1$  most accurate available surfaces. The aug-cc-pVTZ-33211 surface corrects the values of the minima by a few  $\text{cm}^{-1}$  and improves the long-range domain, where differences up to 60  $\text{cm}^{-1}$  are found with respect to the aug-cc-pVDZ-33211 IPES.

Using the potential, the intermolecular level structure of the complex is evaluated and the results compared to those for the aug-cc-pVDZ-33211 CCSD(T) IPES,<sup>13</sup> the empirically derived IPES of ref 10 and the experimental data available.<sup>11,12</sup> The new CCSD(T) IPES gives very accurate results, and handles states with nonzero bending quanta better than does the empirical IPES. The rotational constants of the two benzene–Ar isotopomers are also evaluated and the calculated  $0_0$  values agree well with the experimental values.

**Acknowledgment.** This work has been supported by the Ministerio de Ciencia e Innovación and FEDER (CTQ2005-01076 and CTQ2008-01861/BQU projects and BES-2006-12114 FPI Grant) and by Xunta de Galicia and FEDER (Axuda para Consolidación e Estruturación de Unidades de Investigación Competitivas do Sistema Universitario de Galicia 2007/050 and 2007–2013). We acknowledge computer time from CESGA.

**Supporting Information Available:** CCSD(T) aug-cc-pVTZ-33211 *ab initio* interaction energies,  $V_a$ , and errors of the analytic potential function V-390.  $\text{cm}^{-1}$  fitted to  $V_a$ . Coordinates in Å and energies in  $\text{cm}^{-1}$  (see text for coordinate system). This material is available free of charge via the Internet at <http://pubs.acs.org>.

## References and Notes

- (1) Bartell, L. S. *Chem. Rev.* **1986**, *86*, 491.
- (2) Casassa, M. P. *Chem. Rev.* **1988**, *88*, 815.
- (3) Castleman, A. W., Jr.; Hobza, P. *Chem. Rev.* **1994**, *94*, 1721.
- (4) Weber, Th.; Riedle, E.; Neusser, H. J.; Schlag, E. W. *Chem. Phys. Lett.* **1991**, *183*, 77.
- (5) Leutwyler, S.; Bösiger, J. *Chem. Rev.* **1990**, *90*, 489.
- (6) Weber, Th.; Neusser, H. J. *J. Chem. Phys.* **1991**, *94*, 7689.
- (7) Weber, Th.; von Bargaen, A.; Riedle, E.; Neusser, H. J. *J. Chem. Phys.* **1990**, *92*, 90.
- (8) Koch, H.; Fernández, B.; Christiansen, O. *J. Chem. Phys.* **1998**, *108*, 2784.
- (9) Menapace, J. A.; Bernstein, E. R. *J. Phys. Chem.* **1987**, *91*, 2533.
- (10) Brupbacher, Th.; Makarewicz, J.; Bauder, A. *J. Chem. Phys.* **1994**, *101*, 9736.
- (11) Kim, W.; Felker, P. M. *J. Chem. Phys.* **1997**, *107*, 2193.
- (12) Neuhauser, A.; Braun, J.; Neusser, H. J.; van der Avoird, A. *J. Chem. Phys.* **1998**, *108*, 8408.
- (13) Koch, H.; Fernández, B.; Makarewicz, J. *J. Chem. Phys.* **1999**, *111*, 198.
- (14) Cagide Fajín, J. L.; Fernández, B. *Chem. Phys. Lett.* **2005**, *419*, 55.
- (15) Dunning, T. H., Jr. *J. Chem. Phys.* **1989**, *90*, 1007.
- (16) Tao, F. M.; Pan, Y. K. *Mol. Phys.* **1994**, *81*, 507. Tao, F. M.; Pan, Y. K. *J. Chem. Phys.* **1992**, *98*, 4989.
- (17) Tao, F. M. *J. Chem. Phys.* **1994**, *100*, 3645.
- (18) Fernández, B.; Koch, H.; Makarewicz, J. *J. Chem. Phys.* **1999**, *111*, 5922.
- (19) López, J.; Fernández, B.; Koch, H.; Hold, K.; Jørgensen, P. *J. Chem. Phys.* **2003**, *119*, 4762.
- (20) Koch, H.; Christiansen, O.; Kobayashi, R.; Joergensen, P.; Helgaker, T. *Chem. Phys. Lett.* **1994**, *228*, 233.
- (21) Koch, H.; Sánchez, A.; Helgaker, T.; Christiansen, O. *J. Chem. Phys.* **1996**, *104*, 4157.
- (22) Koch, H.; Joergensen, P.; Helgaker, T. *J. Chem. Phys.* **1996**, *104*, 9528.
- (23) Boys, S. F.; Bernardi, F. *Mol. Phys.* **1970**, *19*, 553.
- (24) Felker, P. M.; Neuhauser, D.; Kim, W. *J. Chem. Phys.* **2001**, *114*, 1233.
- (25) Krause, H.; Neusser, H. J. *J. Chem. Phys.* **1993**, *99*, 6278.
- (26) Felker, P. M. *J. Chem. Phys.* **2001**, *114*, 7901.
- (27) Weber, Th.; von Bargaen, H.; Riedle, E.; Neusser, H. J. *J. Chem. Phys.* **1990**, *92*, 90.
- (28) Krause, H.; Neusser, H. J. *J. Chem. Phys.* **1993**, *99*, 6278.
- (29) Riedle, E.; van der Avoird, A. *J. Chem. Phys.* **1996**, *104*, 882.

JP9012174